Research Article

MOLECULAR PAIN

Molecular Pain
Volume 13: 1–11

DOI: 10.1177/1744806917709201
journals.sagepub.com/home/mpx
SAGE

Potentiation of NMDA receptor-mediated synaptic transmission at the parabrachial-central amygdala synapses by CGRP in mice

Yuya Okutsu[1,2], Yukari Takahashi[1], Masashi Nagase[1], Kei Shinohara[1,2], Ryo Ikeda[2] and Fusao Kato[1]

Abstract

The capsular part of the central amygdala (CeC) is called the "nociceptive amygdala," as it receives nociceptive information from various pathways, including monosynaptic input from the lateral part of the parabrachial nucleus (LPB), a major target of ascending neurons in the spinal and medullary dorsal horn. LPB-CeC synaptic transmission is mediated by glutamate but the fibers from the LPB also contain calcitonin gene-related peptide (CGRP) and the CeC is rich in CGRP-binding sites. CGRP might be released in response to strong nociception and activate these CGRP receptors. Though it has been shown that CGRP affects the excitatory postsynaptic current (EPSC) amplitude at this synapse in a manner sensitive to NMDA receptor (NMDA-R) blockers, the effect of CGRP on postsynaptic NMDA-R-mediated current recorded in isolation has never been directly examined. Thus, we evaluated the effects of CGRP on NMDA-R-mediated EPSCs that were pharmacologically isolated in brain slices from naïve mice. CGRP significantly increased the amplitude of EPSCs mediated by NMDA-Rs in a manner dependent on protein kinase A activation, but not that mediated by alpha-amino-3-hydroxy-5-methyl-4-isoxazolepropionic acid receptors, in concentration-dependent and antagonist-sensitive manners. This CGRP-induced potentiation of synaptic NMDA-R function would have a potent impact on the strengthening of the nociception-emotion link in persistent pain.

Keywords

excitatory postsynaptic currents, parabrachial nucleus, nociception-emotion link

Date received: 21 December 2016; revised: 14 March 2017; accepted: 6 April 2017

Background

Nociceptive signals arising from peripheral nociceptors excite ascending neurons in the spinal dorsal horn and spinal nucleus of the trigeminal nerve. The most notable target of the projections from these ascending nociceptive neurons is the lateral part of the parabrachial nucleus (LPB),[1] and the neurons in the LPB then monosynaptically project to the central nucleus of the amygdala (CeA), especially its capsular part (CeC).[2] Because of this direct nociceptive input, which bypasses the thalamocortical route, and of the subsequent neuronal excitation, the CeC is called the "nociceptive amygdala."[3,4] Synaptic transmission at this LPB-CeC synapse is principally glutamatergic[2] and shows robust potentiation in various types of animal models of semi-acute to chronic pain, including nerve injury-induced neuropathic pain,[5] streptozotocin-induced neuropathic pain,[6] arthritis pain,[7] visceral pain,[8] muscle pain,[9] and formalin-induced inflammatory pain.[2]

Calcitonin gene-related peptide (CGRP) is a 37-amino acid peptide that activates a class of G protein-coupled receptors, CGRP1 and CGRP2 receptors (CGRP1-Rs and CGRP2-Rs, respectively).[10–12] While its role in the inflammatory process in peripheral tissues has been well described, its role in the central nervous system remains

[1]Department of Neuroscience, Jikei University School of Medicine, Minato-ku, Tokyo, Japan
[2]Department of Orthopaedic Surgery, Jikei University School of Medicine, Minato-ku, Tokyo, Japan

Corresponding author:
Fusao Kato, Department of Neuroscience, Jikei University School of Medicine, 3-25-8 Nishi-Shimbashi, Minato, Tokyo 105-8461, Japan.
Email: fusao@jikei.ac.jp

only poorly identified.[13] The LPB is one of the sites with the densest CGRP expression and the CeA is one of the sites with the most CGRP-binding sites and highest CGRP1 receptor expression.[14–17] CGRP-containing terminals arising from the LPB mostly form asymmetrical synapses with CeC neurons[18,19], and optogenetic activation of these terminals gives rise to monosynaptic postsynaptic responses in CeC neurons,[2] which form most monosynaptic LPB-CeC projections underlying nociception-induced threat learning.[20,21] Functionally, microinjection of CGRP1-R antagonists into the CeA of arthritic rats attenuates pain-related behaviors and noxious stimulation-induced responses of CeC neurons.[7] In line with this, application of CGRP antagonists attenuates the potentiated LPB-CeC synaptic transmission in slices acutely prepared from arthritic rats,[7] suggesting that activation of CGRP1-Rs in CeC neurons by CGRP released from the LPB-CeC terminals would play a role in LPB-CeC synaptic potentiation in arthritic rats. In addition, in slices from naïve rats, the LPB-CeC synaptic transmission is potentiated by application of exogenous CGRP.[22] Han et al.[22] attributed the increased excitatory postsynaptic current (EPSC) amplitude after CGRP application to attenuation of the outward rectification property of N-methyl-D-aspartate (NMDA) receptors (NMDA-Rs), resulting in a detectable NMDA receptor-mediated current even at a near-resting holding potential that would otherwise be faint because of its "Mg^{2+}-block" property. However, they did not examine whether the NMDA-R- and alpha-amino-3-hydroxy-5-methyl-4-isoxazolepropionic acid (AMPA) receptor-mediated components at the LPB-CeC synapse recorded in isolation are affected by CGRP. This information is necessary to understand the nature of the effect of CGRP on LPB-CeC synaptic transmission. A recent study indicated that the NMDA-R-mediated synaptic transmission between the basolateral amygdala (BLA) and the CeA is potentiated by CGRP in rat.[23] In this study, we examined whether CGRP affects NMDA-R-mediated postsynaptic currents without affecting AMPA-R-mediated currents at LPB-CeC synapses in isolated brain slices prepared from naïve mice.

Materials and methods

Preparation of transverse brain slices

The protocols of the animal experiments were reviewed and approved by the Institutional Animal Care and Use Committee of Jikei University and conformed to the Guidelines for the Proper Conduct of Animal Experiments of the Science Council of Japan (2006). Transverse slices containing the amygdala from male C57BL/6J mice (14–40 days old) were prepared according to methods described previously.[5,24,25] Briefly, a transverse block of the forebrain containing the amygdaloid complex was dissected out and cut at the midline. The dissected hemisphere was secured on the cutting stage of a vibrating blade slicer (DSK-1000; Dosaka EM) with the rostral end upwards. Coronal slices of 400-μm thickness containing the amygdala were cut in ice-cold cutting artificial cerebrospinal fluid (ACSF) composed of (in mM) 125 NaCl, 3 KCl, 0.1 $CaCl_2$, 5 $MgCl_2$, 1.25 NaH_2PO_4, 10 D-glucose, 0.4 L-ascorbic acid, and 25 $NaHCO_3$ (pH 7.4 bubbled with 95% O_2 + 5% CO_2; osmolarity, approximately 310 mOsm/kg). The slices were first incubated in a holding chamber with a constant flow of standard ACSF, with concentrations of $CaCl_2$ and $MgCl_2$ of 2 mM and 1.3 mM, respectively, at 37°C for 30 to 45 min. The slices were kept at room temperature (about 25°C) in the same chamber until electrophysiological recording. Each slice was transferred to a recording chamber (approximately 0.4 ml volume) and fixed with nylon grids to a platinum frame. The slice was submerged in and continuously superfused at a rate of 1–2 ml/min with the following types of ACSF: (1) *Mg-free ACSF* (mM): 125 NaCl, 3 KCl, 2 $CaCl_2$, 0 $MgCl_2$, 1.25 NaH_2PO_4, 10 D-glucose, 25 $NaHCO_3$, 0.4 L-ascorbic acid, 0.01 CNQX (6-cyano-7-nitroquinoxaline-2,3-dione), and 0.1 picrotoxin; (2) *Low Mg ACSF* (mM): 125 NaCl, 3 KCl, 2 $CaCl_2$, 0.1 $MgCl_2$, 1.25 NaH_2PO_4, 10 D-glucose, 25 $NaHCO_3$, 0.4 L-ascorbic acid, 0.01 CNQX, and 0.1 picrotoxin; (3) *Standard Mg ACSF* (mM): 125 NaCl, 3 KCl, 2 $CaCl_2$, 1.3 $MgCl_2$, 1.25 NaH_2PO_4, 10 D-glucose, 25 $NaHCO_3$, 0.4 L-ascorbic acid, 0.01 CNQX, and 0.1 picrotoxin; and (4) *AMPA-R-recording ACSF* (mM): 125 NaCl, 3 KCl, 2 $CaCl_2$, 1.3 $MgCl_2$, 1.25 NaH_2PO_4, 10 D-glucose, 25 $NaHCO_3$, 0.4 L-ascorbic acid, 0.05 APV (D(−)-2-Amino-5-phosphonopentanoic acid), and 0.1 picrotoxin. The pH was 7.4 when saturated with 95% O_2 + 5% CO_2 and the osmolarity was about 330 mOsm/kg for all of these solutions.

Patch-clamp recordings

Neurons in the CeC were visually identified under an upright microscope (BX-50WI and BX-51WI; Olympus). Whole-cell transmembrane current was recorded from neurons in the CeC of either side. Patch-clamp electrodes were made from borosilicate glass pipettes (1B120F-4; World Precision Instruments). The compositions of the internal solutions were (in mM) as follows: (1) for recordings at a fixed holding potential (−60 mV): 120 K-gluconate, 6 NaCl, 1 $CaCl_2$, 2 $MgCl_2$, 12 Na_2 phosphocreatine, 2 Mg ATP, 0.5 Na GTP, 5 EGTA, and 10 HEPES 1/2Na (pH 7.2 as adjusted with KOH; osmolality; about 300 mOsm/kg); and (2) for plotting the I–V curve of the $EPSC_{NMDA}$: 136 CsCl, 1 $CaCl_2$, 2 Mg ATP, 5 EGTA, 12 Na_2 phosphocreatine, 10 HEPES 1/2Na, and 5 QX-314 (pH 7.3 as

adjusted with CsOH; osmolarity, about 300 mOsm/kg). With these solutions, the tip resistance of the electrode was 4–10 MΩ. The evoked $EPSC_{NMDA}$ or $EPSC_{AMPA}$ were recorded at a holding potential of −60 mV, except during the I–V curve experiments. The input resistance, resting membrane potential, and whole-cell capacitance were measured immediately after the establishment of whole-cell mode by membrane rupture. The membrane response to a rectangular pre-pulse delivered before afferent stimulations was continuously recorded and recordings with fluctuations of series resistance larger than about 30% were discarded. For the I–V curve experiments, the $EPSC_{NMDA}$ was recorded at holding potentials from −70 mV to +35 mV with the protocol described below. Membrane currents were recorded using a Axopatch 200B and a Multiclamp 700B amplifier (Molecular Devices), low-pass filtered at 2 kHz, and digitized at 10 kHz and with a 16-bit resolution with a PowerLab interface (ADInstruments).

All recordings were made at room temperature (about 25°C). All compounds except those noted were purchased from Sigma-Aldrich Japan (Tokyo, Japan), Wako Pure Chemical Industries (Osaka, Japan), and Nacalai Tesque (Kyoto, Japan).

Estimation of the I–V relationship of the $EPSC_{NMDA}$

The protocol used to estimate the I–V relationship of the $EPSC_{NMDA}$ is illustrated in Figure 3(a.1). First, the membrane potential of neurons was held at −70 mV for 10 s and a pre-pulse (PP, arrow; 50 ms, −5 mV) was delivered to measure relative changes in membrane properties. After a pause of 200 ms, four pulses of electrical stimulation were delivered with 10-s intervals. The four responses to each of these stimuli were used to calculate the average wave form of the $EPSC_{NMDA}$. After a pause of 5 s following the last stimulation, the membrane potential (V_m) was gradually depolarized to −35 mV for 20 s and kept at −35 mV. A pause of 10 s was given at −35 mV before starting the four stimuli. This epoch composed of 10-s pause, 4 stimuli at 10-s interval (shown as short vertical bars in Figure 3(a.1)), and 5 s pause after the last stimulus was repeated at −35, 0, and +35 mV with gradual shift of the holding potential from 1 s to another for 20 s in-between. After the last stimulation at +35 mV, the V_m was slowly shifted back to −70 mV for 30 s. Single episode of voltage clamps and stimulations took 280 s and repeated every 5 min. Thus, the $EPSC_{NMDA}$ waveforms (average of 4 consecutive responses) at −70 mV, −35 mV, 0 mV, and +35 mV were obtained every 5 min.

Afferent pathway stimulation

A bipolar steel electrode (interpolar distance, approximately 100 μm; Unique Medical, Tokyo, Japan) was carefully placed on the fiber tract ventromedial to the CeC under microscopic control to stimulate the LPB pathway, and the stimulation intensity was set so that the $EPSC_{AMPA}$ amplitude became approximately 100 pA before CNQX application. The resulting stimulation intensity was 0.1–1 mA (average, 0.62 mA). The pulse duration was 100 μs. During the $EPSC_{AMPA}$ recordings, double pulses with an inter-stimulus interval of 100 ms were delivered to calculate the paired-pulse ratio (PPR) of the $EPSC_{AMPA}$ amplitude by normalizing the amplitude of the second one by that of the first one.[5]

Drug application

CGRP and BIBN4096BS, a selective non-peptide CGRP1 receptor antagonist,[26] were dissolved in ACSF. BIBN4096BS was a kind gift from Boehringer-Ingelheim, Japan. KT5720 was obtained as a solution at 10 mM in DMSO (Tocris, Bristol, UK) and dissolved in ACSF at the final concentration (1 μM). For the CGRP application in the presence of KT5720, CGRP solution (500 nM) was made with the ACSF containing KT5720 at 1 μM.

Data and statistical analysis

The recorded membrane current was analyzed off-line with Igor Pro 6 (WaveMetrics, OR, USA) using procedures written by FK. Peak amplitude was measured on the basis of the averaged waveform of the evoked EPSCs (average times are noted for each result). Values are expressed as mean values ± standard error of the mean. Differences in values were compared using one-way analysis of variance (ANOVA) followed by a post hoc test (Gabriel test) two-way ANOVA, Student's t test, or Mann–Whitney U test. Differences with a probability (P) less than 0.05 were considered significant.

Results

CGRP increases the $EPSC_{NMDA}$ with a slow time course

First, we applied 500 nM CGRP onto slices containing the CeC for 20 min while recording the postsynaptic NMDA receptor-mediated current ($EPSC_{NMDA}$) in response to LPB pathway stimulation. The NMDA component was pharmacologically isolated by the addition of CNQX (10 μM) and picrotoxin (100 μM) and the membrane potential was kept at −60 mV in the presence of 2 mM Ca^{2+} and 0 mM Mg^{2+}. This ACSF solution was perfused for more than 10 min before the application of CGRP. At the end of the recording, APV (50 μM) was applied to confirm the NMDA-R-mediated current.

Application of CGRP (500 nM) slowly increased the amplitude of the $EPSC_{NMDA}$ (Figure 1(a.1), (b.1), and (c.1)) with little effect on its kinetics. Interestingly, the gradual increase in amplitude was still observed even after washout for >30 min (Figure 1(c.1)). Approximately half of the neurons showed a manifest response to CGRP with an increase in the $EPSC_{NMDA}$ (Figure 1(a.1), (b.1), and (c.1)), whereas the other neurons showed relatively smaller responses to CGRP (results from a representative neuron are shown in Figure 1(a.2), (b.2), and (c.2)). Sustained perfusion of the same ACSF not containing CGRP for 50 min (this is indicated as "0 CGRP" in Figure 1(a.3), (b.3), and (c.3), to facilitate comparison with "500 CGRP") did not markedly affect or only slightly affected the amplitude of the $EPSC_{NMDA}$ (Figure 1(a.3), (b.3), and (c.3)). In all cases with APV application (20 neurons from 19 mice), the $EPSC_{NMDA}$ was almost completely abolished with 50 μM APV ("7" in Figure 1(a) and "APV" in Figure 1(b) and (c)).

The changes in the $EPSC_{NMDA}$ amplitude for 12 neurons after 20-min application of CGRP followed by 10-min washout are summarized in Figure 1(d). Based on the 99% confidence limit (horizontal dotted line in Figure 1(d)) of the "Control" effects (black open circles), we classified the neurons as "responders" to CGRP (blue circles in Figure 1(d)) or "non-responders" (red circles in Figure 1(d)). There was significant difference ($P < 0.01$; one-way ANOVA with post hoc Gabriel test) between the mean $EPSC_{NMDA}$ amplitudes for responders and control (0 CGRP) but not between those for the control and non-responders.

We then examined the effect of CGRP (500 nM) in the presence of protein kinase A (PKA) inhibitor KT5720 (1 μM), which was applied from 15 to 20 min before the application of CGRP and present in the ACSF during whole span of recording. The X markers in Figure 1(d) indicate $EPSC_{NMDA}$ amplitude after 10 min wash after 20 min application of CGRP as with the data shown with open circles but recorded in the presence of KT5720. There were significant differences ($P < 0.01$; one-way ANOVA with post hoc Gabriel test) between the mean $EPSC_{NMDA}$ amplitude for responders and that recorded in the presence of KT5720 but not between that for the non-responders and that recorded in the presence of KT5720 (Figure 1(d)). These results suggest activation of PKA plays a significant role in the effect of CGRP in augmenting $EPSC_{NMDA}$.

Figure 1(e) shows the time course of the $EPSC_{NMDA}$ amplitude of responders (blue circles) and non-responders (red circles) to 500 nM CGRP (horizontal bar) and to control solution (black circles). One-way ANOVA analysis indicated that there were significant differences between these three groups at every time point after 15 min ($F(2,20) = 4.48$ and $P = 0.025$ for 15 min and $F(2,17) = 5.76$ and $P = 0.012$ for 50 min (recording was discontinued before 50 min for two neurons in the control group and one neuron in the non-responder group); $P < 0.05$ at all other time points), and post hoc analysis (Gabriel test) indicated that there were significant differences between the $EPSC_{NMDA}$ amplitudes in responder neurons and control and non-responder neurons after 15 min ($P = 0.044$ and 0.042 at 15 min; $P = 0.020$ and 0.032 at 50 min; $P < 0.05$ at all other time points; Gabriel test). These were designated "responding" and "non-responding" neurons, respectively. The increased $EPSC_{NMDA}$ amplitude in responding neurons did not recover after 30 min of washout (Figure 1(e)) and was still increasing (Figure 1(e)). Unlike the impression from the representative traces in Figure 1(a.1) and (a.2), the amplitude and decay kinetics of the $EPSC_{NMDA}$ were not apparently related to the difference in responses to CGRP in each neuron. There were no significant differences in the peak amplitude and decay kinetics between these two groups (peak amplitude, 25.3 pA ± 15.3 pA and 40.5 ± 19.2 pA ($P = 0.22$; Mann–Whitney U test); decay time constant, 75.7 ms ± 41.6 ms and 64.5 ms ± 28.8 ms ($P = 0.75$; Mann–Whitney U test) for responders ($n = 6$) and non-responders ($n = 6$), respectively).

Interestingly, the $EPSC_{NMDA}$ amplitude increased slightly but significantly during the course of recording with low Mg^{2+} concentration (0 mM for data in Figure 1 and 0.1 mM for data in Figure 2). This increase was significant between the amplitude at time 0 (Figure 1(e) and 2(a)) and that at any time point thereafter (point-to-point comparison with Mann–Whitney U test; $P < 0.05$). As such gradual increase in $EPSC_{NMDA}$ amplitude was similarly observed even in the 0 CGRP groups and was not observed with $EPSC_{AMPA}$ (Figure 4(c)), it is unlikely that this increase resulted from the CGRP effect but rather it might have resulted from repeated activation of NMDA-Rs in the environment containing low concentration of Mg^{2+}. The mechanism underlying this increase was not further examined.

The increase in the $EPSC_{NMDA}$ amplitude by CGRP is concentration-dependent and mediated by CGRP1 receptors

Figure 2(a) shows the responses of the $EPSC_{NMDA}$ to different concentrations of CGRP recorded in the presence of 0.1 mM Mg^{2+}, a low Mg condition almost similar to that used for the experiments in Figure 1. In this experiment, we did not distinguish responders and non-responders and simply compared pooled responses to applications of control (i.e., 0 nM CGRP), 100 nM, 250 nM, and 500 nM CGRP for 20 min. Figure 2(a.2) indicates the time course of the $EPSC_{NMDA}$ amplitude before, during, and after CGRP application. Two-way ANOVA revealed that there were significant effects of concentration and time ($F(35,396) = 4.120$;

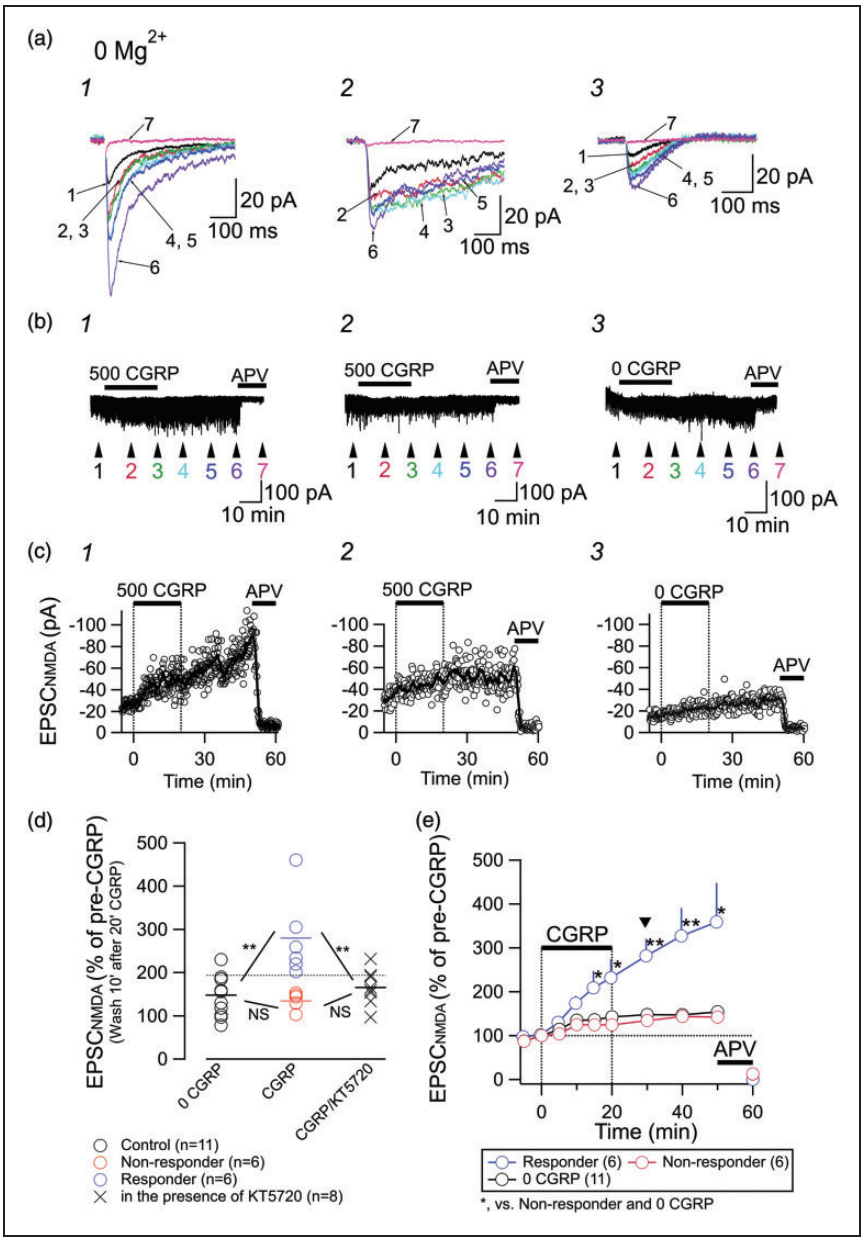

Figure 1. Effect of CGRP on the postsynaptic NMDA-R-mediated current. (a) Representative traces showing $EPSC_{NMDA}$ waveforms evoked by LPB pathway stimulation recorded in the absence of Mg^{2+}, in the presence of CNQX, and at a holding potential of −60 mV. Traces with numbers 1–7 are the averaged waveforms of 20 consecutive responses sampled at the time points 1–7 indicated in (b). 1, responder; 2, non-responder; 3, recordings from a neuron to which no CGRP was applied. (b) Representative recordings of the membrane current in CeC neurons. Numbers 1–7 show the time points for the averaged waveforms in (a). Drugs (CGRP (500 nM for 1 and 2; 0 nM for 3) and APV (50 μM)) were bath-applied for the indicated times (horizontal bars). Stimulation artifacts and pre-pulse are removed. (c) Representative examples of the time course of the $EPSC_{NMDA}$ amplitude (open circles, the amplitude of each $EPSC_{NMDA}$; thick curves, moving average over nine consecutive responses). (d) Changes in the $EPSC_{NMDA}$ amplitude at 10 min after the cessation of the 20-min application of CGRP. "0 CGRP," continued application of ACSF not containing CGRP; "CGRP," application of 500 nM CGRP (at the 10-min washout after 20-min application); "CGRP/KT5720", application of 500 nM CGRP in the sustained presence of 1 μM KT5720. The horizontal dotted lined shows the upper 99% confidence limit of the responses of 11 neurons receiving no CGRP (black open circles). The neurons showing larger responses than this limit were classified as "responders to CGRP." ** $P < 0.01$; one-way ANOVA with post hoc Gabriel test. (e) Summary of the time course of the $EPSC_{NMDA}$ amplitude. CGRP (0 or 500 nM) and APV (50 μM) were applied at the horizontal bars. Arrowhead indicates the time point for the value measurement used in panel (d). *$P < 0.05$, **$P < 0.01$; Mann–Whitney U test (CGRP (500 nM) was compared with control ("0 CGRP")). Error bars represent mean ± SEM.

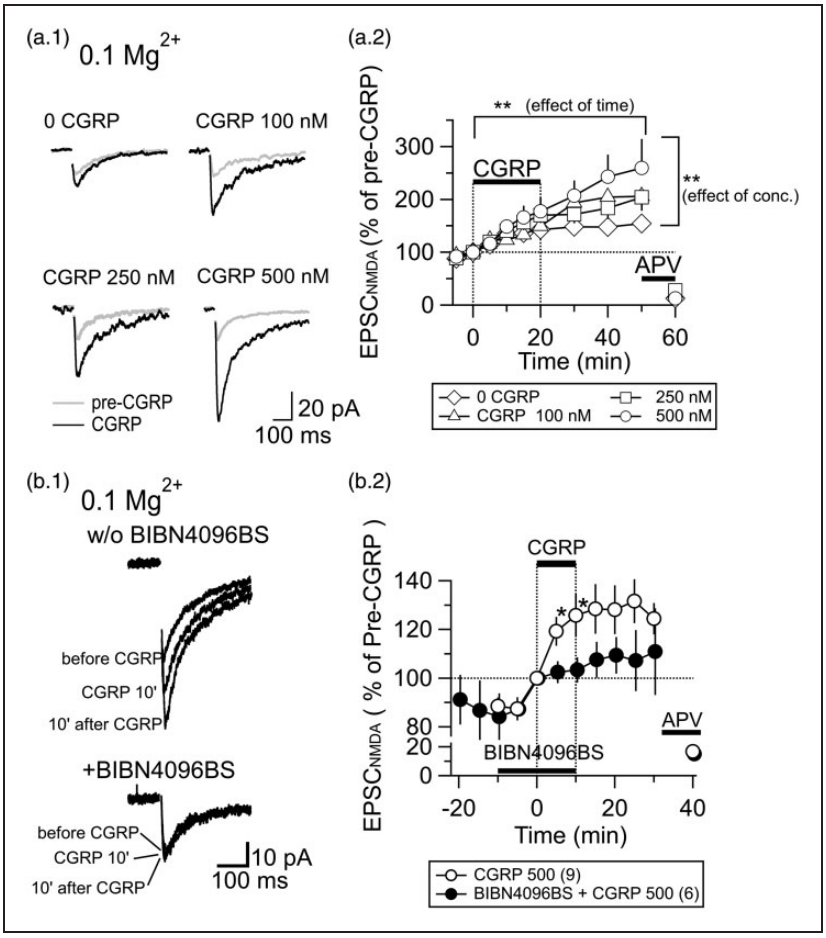

Figure 2. The increase in the $EPSC_{NMDA}$ amplitude by CGRP is concentration-dependent and mediated by CGRP1 receptors. (a.1) Traces showing $EPSC_{NMDA}$ waveforms (average of 20 consecutive traces) evoked by LPB pathway stimulation. "Pre-CGRP," before application of CGRP; "CGRP," after 20-min application of CGRP (0–500 nM). (a.2) The time course of the $EPSC_{NMDA}$ amplitude in response to the application of different concentrations of CGRP (0–500 nM; see legend at the bottom for the concentration). CGRP and APV (50 μM) were applied at the horizontal bars. Error bars represent mean ± SEM. Two-way ANOVA (see text for details). (b.1) Traces showing $EPSC_{NMDA}$ waveforms (average of eight consecutive traces) evoked by LPB pathway stimulation. "w/o BIBN4096BS," without BIBN4096BS; "+BIBN4096BS," in the presence of BIBN4096BS; "before CGRP," before application of CGRP; "CGRP 10'," at 10-min application of CGRP (500 nM, 10 min); "10' after CGRP", 10 min after the cessation of the 10-min application of CGRP. (b.2) Time course of the effects of CGRP (500 nM) on the $EPSC_{NMDA}$ amplitude measured in the presence and absence of BIBN4096BS (1 μM). *$P < 0.05$; Mann–Whitney U test. Error bars represent mean ± SEM. Application of APV confirmed the NMDA-R-mediated component. CGRP, BIBN4096BS, and APV were applied at the horizontal bars. The numbers in the parenthesis in the legend show the number of neurons.

$F(8) = 13.304$, $P < 0.001$ for time; $F(3) = 4.638$, $P = 0.003$ for concentration) without significant interaction between time and concentration ($F(24) = 0.661$; $P = 0.889$), suggesting that the effect of CGRP on the $EPSC_{NMDA}$ amplitude is time- and concentration-dependent.

To identify the type of receptors involved in the effects of CGRP, we compared the effects of CGRP on the $EPSC_{NMDA}$ amplitude recorded in isolation at −60 mV with 0.1 mM Mg^{2+} between CGRP applied in the presence and absence of non-peptide CGRP1-R antagonist. BIBN4096BS (1 μM) was bath-applied for 10 min before the application of 500 nM CGRP solution, which also contained the same concentration of the antagonist (Figure 2(b.1)). In the presence of BIBN4096BS, CGRP only slightly affected the $EPSC_{NMDA}$ (Figure 2(b.2)). There was a significant difference in the $EPSC_{NMDA}$ amplitude with CGRP between that in the presence and absence of BIBN4096BS after 5 min and 10 min of CGRP application (*$P < 0.05$; Mann–Whitney U test; Figure 2(b.2)). An interesting observation with this 10-min application of 500 nM CGRP (Figure 2(b.2)) compared with the 20-min application (Figure 2(a.2)) was that the sustained increase in $EPSC_{NMDA}$ even after >20 min washout was not manifested with the 10-min application. It is therefore possible that the prolonged potentiating effect of CGRP on $EPSC_{NMDA}$ might depend on the

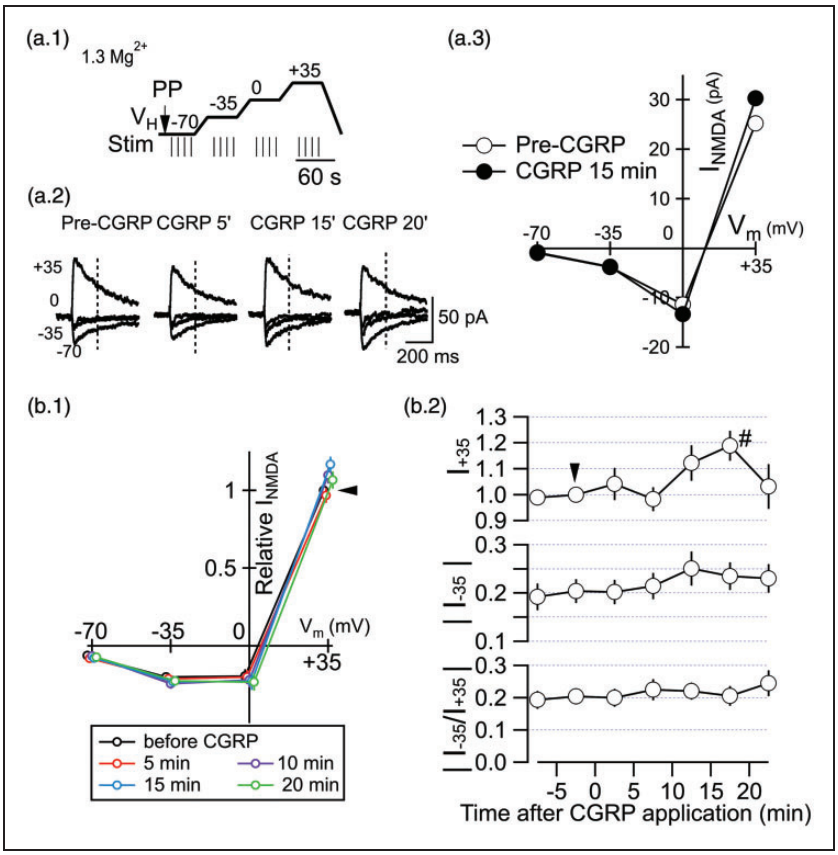

Figure 3. CGRP has little effect on the membrane potential-dependence of the $EPSC_{NMDA}$. (a.1) Schema showing the voltage-clamp command protocol used to analyze the holding potential-dependency of the $EPSC_{NMDA}$ (see the Materials and methods section for details). The LPB fibers were stimulated four times at each of the voltage steps (short vertical bars at 10-s intervals). The responses to the four stimuli at each voltage step were averaged. PP, pre-pulse application, with which changes in series resistance was monitored. Each episode composed of voltage steps and stimulations took 280 s and repeated every 5 min to obtain averaged $EPSC_{NMDA}$ waveforms at 5-min interval (as shown in Figure 3(a.2)). (a.2) Traces showing $EPSC_{NMDA}$ waveforms (average of four consecutive traces) evoked by LPB pathway stimulation at −70, −35, 0, and +35 mV holding potentials using the protocol in Figure 3(a.1). "Pre-CGRP," before application of CGRP; "CGRP 5'," "CGRP15'," and "CGRP 20'," indicate those at 5, 15, and 20 min after the initiation of CGRP application (500 nM), respectively. (a.3) Current–voltage relation of the $EPSC_{NMDA}$ at pre-CGRP (open circles) and 15 min after CGRP (500 nM; filled circles). The amplitude of the $EPSC_{NMDA}$ current was measured 200 ms after the stimulation (vertical dashed line in (a.2)). (b.1) The $EPSC_{NMDA}$ amplitude–voltage relation at before CGRP, CGRP 5 min, 10 min, 15 min, and 20 min. The $EPSC_{NMDA}$ amplitude was measured 200 ms after the stimulation. The black arrowhead shows the relative $EPSC_{NMDA}$ current at +35 mV before CGRP application with which all other amplitudes are normalized. (b.2) The time course of the $EPSC_{NMDA}$ amplitude (top, measured at a V_H of +35 mV (relative to the $EPSC_{NMDA}$ amplitude at a V_H of +35 mV at pre-CGRP); middle, that at −35 mV; bottom, the absolute value of the ratio of the $EPSC_{NMDA}$ amplitude at −35 mV to that at +35 mV). CGRP (500 nM) was applied from around 0 min for 20 min (note that the timing for obtaining $EPSC_{NMDA}$s for distinct holding potentials deviates from the time shown in Figure 3(b.2) by ~2 min at the maximum due to the sequential sampling of the data; Figure 3(a.1)). The $EPSC_{NMDA}$ was recorded with "standard Mg ACSF" containing 1.3 mM Mg^{2+}. The black arrowhead shows the relative $EPSC_{NMDA}$ current at +35 mV before CGRP application with which all other amplitudes are normalized. $^{\#}P < 0.05$ vs. before CGRP; Mann–Whitney U test. Error bars represent mean ± SEM. n = 10 neurons.

duration of the receptor stimulation, which would require more systematic analysis.

CGRP has little effect on the current–voltage relationship of the $EPSC_{NMDA}$

CGRP increases the amplitude of the EPSC recorded as a mixture of the $EPSC_{AMPA}$ and $EPSC_{NMDA}$.[22] In that study, it was interpreted that CGRP attenuated the outwardly rectifying properties of NMDA-Rs (i.e., "Mg^{2+}-block" at hyperpolarized potentials) such that significant $EPSC_{NMDA}$ components became large enough to be observed as an inward current similar to $EPSC_{AMPA}$, even in the presence of 1.2 mM Mg^{2+} at −60 mV.[22] However, the effect of CGRP on the I–V relationship of the $EPSC_{NMDA}$ has never been directly assessed in

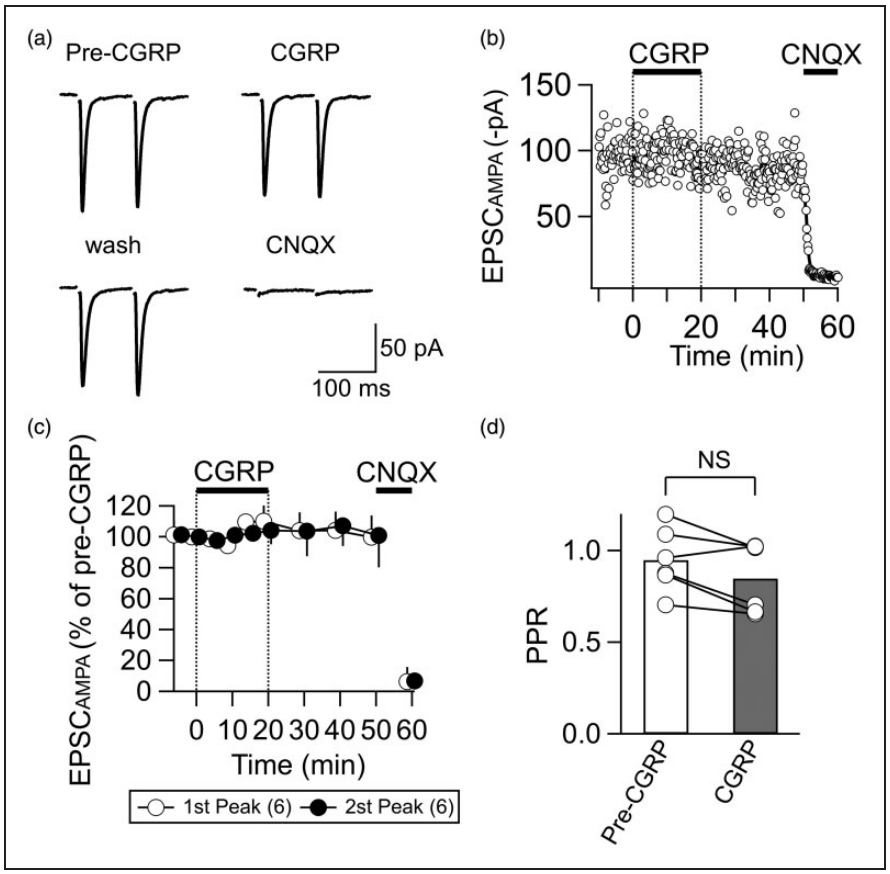

Figure 4. CGRP does not affect the $EPSC_{AMPA}$. (a) Representative traces showing $EPSC_{AMPA}$ waveforms (average of eight consecutive traces) evoked by paired-pulse stimulation at an inter-stimulus interval of 100 ms. CGRP, 20 min after 500 nM CGRP application; wash, 20 min after cessation of CGRP application; CNQX, after 5-min application of CNQX (10 μM). Recording with the "AMPAR-recording ACSF." (b) A representative example of the time course of the $EPSC_{AMPA}$ amplitude (open circle, $EPSC_{AMPA}$ amplitude in response to each stimulation; thick curve, moving average over nine consecutive responses). CGRP (500 nM) and CNQX (10 μM) were applied at the horizontal bars. (c) The summary of the time course of the $EPSC_{AMPA}$ amplitude (normalized by the pre-CGRP value). White and black circles show relative mean amplitudes of the first and second peaks, respectively ($n = 6$). Vertical bars indicate SEM. CGRP (500 nM) and CNQX (10 μM) were applied at the horizontal bars as indicated. (d) Summary of the effects of CGRP (500 nM, 20 min) on the PPR of the $EPSC_{AMPA}$. NS, not significantly different (paired t test). $n = 6$ neurons.

isolation at the LPB-CeC synapse. To directly address this issue, the LPB fibers were repeatedly stimulated at different holding potentials (–70 mV, −35 mV, 0 mV, and +35 mV) four times at 10-s intervals to get the average response at each holding potential (see Methods and Materials section and Figure 3(a.1)) in ACSF solution containing 1.3 mM Mg^{2+}. This external solution allows the appearance of the typical outward rectification of the NMDA-R current. Using the averaged waveform of the $EPSC_{NMDA}$ at four different holding potentials recorded in the presence of CNQX (10 μM), we measured the amplitude of the $EPSC_{NMDA}$ at 200 ms from the stimulus (vertical dotted lines in Figure 3(a.2)) to construct the I–V curve of the synaptically activated NMDA-R responses. Figure 3(a.3) indicates the I–V curve constructed from the representative responses in Figure 3(a.2). Despite an increase in the $EPSC_{NMDA}$ amplitude at +35 mV, there was no apparent change in its amplitude at −70 mV. Figure 3(b) summarizes the voltage-dependency of the $EPSC_{NMDA}$. Figure 3(b.1) shows the mean normalized $EPSC_{NMDA}$ amplitude during the course of CGRP (500 nM) application. This normalized $EPSC_{NMDA}$ amplitude was obtained by dividing the $EPSC_{NMDA}$ amplitude by that before CGRP application recorded at +35 mV. As shown in Figure 3(b.2), despite a significant increase in the normalized $EPSC_{NMDA}$ amplitude at +35 mV at 15 min after application (top curve: $P < 0.05$; Mann–Whitney U test, vs. Pre-CGRP; $n = 10$ neurons), there was almost no changes in the I_{-35}/I_{+35}, a rectification index calculated to evaluate the changes in the outward rectification properties of the $EPSC_{NMDA}$ (the curve at the bottom; $P > 0.05$). These results indicate that CGRP increases the $EPSC_{NMDA}$

recorded in isolation without significantly affecting the outward rectification property of the NMDA-Rs in the presence of 1.3 mM Mg^{2+}.

CGRP does not affect the $EPSC_{AMPA}$ amplitude

It is most likely that the increase in the $EPSC_{NMDA}$ amplitude induced by CGRP resulted from a direct effect on NMDA-R functions. However, such an increase would also occur through (1) an increased release of glutamate, (2) decreased intracleft clearance of glutamate, or (3) any other changes resulting in a general increase in glutamatergic signaling (e.g., an increase in energy supply[27]). To examine these possibilities, we analyzed the effect of CGRP on the AMPA receptor-mediated EPSC ($EPSC_{AMPA}$). The $EPSC_{AMPA}$ was recorded in isolation in ACSF containing 1.3 mM Mg^{2+}, 2 mM Ca^{2+}, 0.05 mM APV, and 0.1 mM picrotoxin at a holding potential of −60 mV. Application of CGRP for 20 min did not significantly affect the amplitude of the $EPSC_{AMPA}$ (Figure 4(a), (b), and (c); paired t test). These $EPSC_{AMPA}$ components were mediated by postsynaptic AMPA receptors because CNQX completely abolished this component (Figure 4(a), (b), and (c); CNQX). Also, the PPR of the $EPSC_{AMPA}$ amplitude in response to paired stimulation at an interval of 100 ms was not affected by CGRP (Figure 4(a) and (d); paired t test). These results indicate that CGRP does not affect postsynaptic AMPA receptors and the glutamate release probability; rather, it is likely that this increase in the $EPSC_{NMDA}$ resulted from a direct enhancing effect of CGRP on NMDA-Rs.

Discussion

The LPB is the site with the highest expression of CGRP in the whole brain, and the CeA, particularly the CeC and CeL, has a very high density of terminals containing CGRP in mice and rats.[16,18] CGRP-binding sites are also rich in the CeA.[15] These terminals arising from the LPB form asymmetric synapses at the dendritic shafts of CeC neurons.[18,19] Thus, it is postulated that co-released CGRP would modulate excitatory synaptic transmission at these LPB-CeC synapses. In agreement with this, it has been shown that exogenous application of CGRP increases the amplitude of the LPB-CeC EPSC recorded as a mixture of AMPA-R- and NMDA-R-mediated currents at −60 mV, and this increase was not observed in the presence of APV.[22] However, it remained unclear whether CGRP could affect the NMDA-R-mediated current itself, because the recordings in their report comprised a mixture of these two types of glutamate receptor-mediated currents.

In the present study, we have clearly demonstrated that exogenously applied CGRP significantly increases the amplitude of the $EPSC_{NMDA}$ recorded in isolation at the LPB-CeC synapses in a dose-dependent manner. This increase was characterized by the following: (1) it was observed in the absence of Mg^{2+} block, unlike in the report by Han et al.;[22] (2) it was inhibited by a CGRP1 receptor antagonist; (3) it continued to develop slowly even after the agonist washout particularly after longer application; (4) this increase was significantly attenuated when activation of PKA is inhibited, thus suggesting an involvement of PKA-dependent process; (5) it was not accompanied by a significant change in the voltage dependency of the $EPSC_{NMDA}$ recorded in the presence of 1.3 mM Mg^{2+}; and (6) CGRP exerted no effects on the amplitude of the $EPSC_{AMPA}$ and release probability of glutamate from the terminal of LPB fibers. Such selective enhancement of NMDA-R-mediated components might play a role in the activity-dependent potentiation of LPB-CeC synapses observed in chronic pain models.[2,5,6,8,24]

CGRP affects NMDA receptor function

A recent study indicated that exogenous CGRP increases the current through subsynaptic NMDA receptors at BLA-CeA synapses.[23] The present study adds a novel finding that CGRP induces synaptic potentiation not only at the BLA-CeA synapse but also at the LPB-CeC synapse in a manner, at least partly, dependent on PKA activation. This finding is of interest because (1) the BLA-CeA projection itself does not contain CGRP[18] and (2) we have demonstrated that both BLA-CeA and LPB-CeC pathways show manifest synaptic potentiation following fear/threat learning.[25] A plausible scenario is that the activation of CGRP1-Rs by CGRP released from the LPB terminals affects NMDA-Rs expressed in the same neurons through unidentified intracellular mechanisms. It is therefore an interesting future project to directly demonstrate whether CGRP is indeed released from the stimulated terminals with the stimulation pattern used in this study to stimulate glutamate release or CGRP is released only in response to specific stimulation pattern or intensity.

The CGRP1-Rs are formed as a heterodimeric complex composed of a G protein-coupled receptor and an accessory protein RAMP1 and are usually coupled with G_s proteins. Thus, activation of CGRP receptors increases cAMP production and activates protein kinase A. As the increase in the isolated NMDA-R-mediated EPSC amplitude by CGRP in the absence of Mg^{2+} blockade in the present study was significantly attenuated by PKA inhibition in a similar manner to the reported PKA-dependent increase in the EPSC amplitude that was dependent on Mg^{2+} block relief,[22] both effects are likely to be downstream to the G_s-mediated activation of PKA by CGRP1-R stimulation. Notably, PKA activation or phosphorylation leads to increased

channel opening probability and increased subsynaptic membrane trafficking of NMDA receptors.[28–30] This positive regulation of NMDA-R function by CGRP is in agreement with the increase in the $EPSC_{NMDA}$ amplitude in this study.

Han et al.[22] attributed the increase in the amplitude of the EPSC recorded as a mixture of AMPA-R- and NMDA-R-mediated components by CGRP at the LPB-CeC synapse to the decreased rectification of PKC-activated NMDA-R reported in trigeminal neurons and faster kinetics of NR1/NR2C receptors in heterologously expressed NMDA-Rs with a phosphorylation-mimicking point mutation.[31,32] However, the CGRP-sensitive $EPSC_{NMDA}$ observed in the present study showed much slower rise and decay kinetics than the $EPSC_{AMPA}$ both before and after CGRP application, making it unlikely that the $EPSC_{NMDA}$ becomes indistinguishable from $EPSC_{AMPA}$, even after CGRP application. Of note, Wu et al.[23] attributed the long-lasting synaptic potentiation of the field EPSP slope of BLA-CeA transmission after the application of CGRP in slices to a secondary effect of the CGRP-induced enhancement of postsynaptic NMDA currents. Although it remains to be demonstrated whether such potentiation also occurs at LPB-CeC synapses, a possible cause of the increase in the EPSC amplitude reported in a previous paper[23] would be such NMDA-R-dependent secondary potentiation of AMPA-R function. In addition to this possibility, the differences in the experimental conditions, such as the difference in the species, the recording temperature and the age of the animals, would also underlie the differences between our data and those of the previous report.[22] However, the absence of the change in the $EPSC_{AMPA}$ amplitude following CGRP application commonly observed in the study by Han et al.[22] (recording at 31°C), by Wu et al.[23] (at room temperature), and in this study (at room temperature) would suggest that the lower temperature used in this study and that by Wu et al.[23] would not resulted in the absence of this CGRP effect.

Functional significance of the synaptic modulation by CGRP

The behavioral effect and roles of CGRP in the amygdala complex remain controversial. Han et al.[22] reported that intra-CeA injection of CGRP in awake rats augments nociception-induced responses. In contrast, CGRP microinjected into the CeA[33] and BLA[17] of anesthetized rats exerts analgesic effects. Because the CeA is mostly composed of inhibitory neurons, which are mutually interconnected to form a circuit with complex feedforward and feedback inhibitions (discussed in Ehrlich et al.[34] and Sugimura et al.[2]), the final behavioral outcomes of intra-CeA CGRP-R stimulation would largely depend on the role of the subpopulation of neurons activated by CGRP. In agreement with this, we have recently demonstrated that despite the presence of monosynaptic EPSC in response to selective optogenetic stimulation of the LPB fibers in almost all neurons in the CeC, as confirmed by optogenetic activation of the presynaptic terminals, only the neurons with late-firing properties show potentiated EPSCs at 24 h after intraplantar formalin injection. This suggests that the synaptic plasticity in response to sustained intensive nociceptive inputs is not shared by all of the LPB-CeC synapses.

In conclusion, it is likely that CGRP in the CeA is a peptidergic modulator of synaptic plasticity. Pharmacological intervention in this CGRP system in the CeA would have therapeutic potential for improving fear-/threat-related emotional disorders such as post-traumatic stress disorder[23] but also emotional complications in persistent pain.[35]

Authors' Contributions

FK designed the study and YO, YT, and MN carried out all experiments and data analyses. FK wrote the manuscript and wrote home-made analysis macros and YO, YT, RI, and KS participated in the discussion and made essential contributions to the manuscript. All authors read the final version of the manuscript.

Declaration of Conflicting Interests

The author(s) declared the following potential conflicts of interest with respect to the research, authorship, and/or publication of this article: The authors acknowledge the gift of BIBN4096BS from Boehringer-Ingelheim, Japan. Otherwise, we declare no conflict of interest for the materials and techniques used in this study.

Funding

The author(s) disclosed receipt of the following financial support for the research, authorship, and/or publication of this article: This work was supported by a Grant-in-Aid for Exploratory Research from the Ministry of Education, Culture, Sports, Science, and Technology to F.K. (No. 23650208), MEXT-Supported Program for the Strategic Research Foundation at Private Universities (S1311009) to F.K., a Grant-in-Aid for Scientific Research (B) to F.K. (25293136), the Strategic Research Program for Brain Sciences to F.K. and a Grant-in-Aid for Young Scientists (B) to Y.T. (25860429).

References

1. Todd AJ. Neuronal circuitry for pain processing in the dorsal horn. *Nat Neurosci* 2012; 11: 823–836.
2. Sugimura YK, Takahashi Y, Watabe AM, et al. Synaptic and network consequences of monosynaptic nociceptive inputs of parabrachial nucleus origin in the central amygdala. *J Neurophysiol* 2016; 115: 2721–2739.
3. Neugebauer V, Galhardo V, Maione S, et al. Forebrain pain mechanisms. *Brain Res Rev* 2009; 60: 226–242.

4. Bernard JF, Huang GF and Besson JM. Nucleus centralis of the amygdala and the globus pallidus ventralis: electrophysiological evidence for an involvement in pain processes. *J Neurophysiol* 1992; 68: 551–569.
5. Ikeda R, Takahashi Y, Inoue K, et al. NMDA receptor-independent synaptic plasticity in the central amygdala in the rat model of neuropathic pain. *Pain* 2007; 127: 161–172.
6. Ochiai T, Takahashi Y, Asato M, et al. *Bilateral potentiation of parabrachial, but not basolateral amygdala inputs, to central capsular amygdala neurons in neuropathic diabetic mice*. Program No. 785.03. 2012 Neuroscience Meeting Planner. New Orleans, LA: Society for Neuroscience, 2012. Online.
7. Han J-S, Li W and Neugebauer V. Critical role of calcitonin gene-related peptide 1 receptors in the amygdala in synaptic plasticity and pain behavior. *J Neurosci* 2005; 25: 10717–10728.
8. Han JS and Neugebauer V. Synaptic plasticity in the amygdala in a visceral pain model in rats. *Neurosci Lett* 2004; 361: 254–257.
9. Cheng S-J, Chen C-C, Yang H-W, et al. Role of extracellular signal-regulated kinase in synaptic transmission and plasticity of a nociceptive input on capsular central amygdaloid neurons in normal and acid-induced muscle pain mice. *J Neurosci* 2011; 31: 2258–2270.
10. Tomlinson AE and Poyner DR. Multiple receptors for calcitonin gene-related peptide and amylin on guinea-pig ileum and vas deferens. *Br J Pharmacol* 1996; 117: 1362–1368.
11. Van Rossum D, Hanisch UK and Quirion R. Neuroanatomical localization, pharmacological characterization and functions of CGRP, related peptides and their receptors. *Neurosci Biobehav Rev* 1997; 21: 649–678.
12. Wimalawansa SJ. Calcitonin gene-related peptide and its receptors: molecular genetics, physiology, pathophysiology, and therapeutic potentials. *Endocr Rev* 1996; 17: 533–585.
13. Gungor NZ and Pare D. CGRP inhibits neurons of the bed nucleus of the stria terminalis: implications for the regulation of fear and anxiety. *J Neurosci* 2014; 34: 60–65.
14. D'Hanis W, Linke R and Yilmazer-Hanke DM. Topography of thalamic and parabrachial Calcitonin Gene-Related Peptide (CGRP) immunoreactive neurons projecting to subnuclei of the amygdala and extended amygdala. *J Comp Neurol* 2007; 505: 268–291.
15. Kruger L, Mantyh PW, Sternini C, et al. Calcitonin gene-related peptide (CGRP) in the rat central nervous system: patterns of immunoreactivity and receptor binding sites. *Brain Res* 1988; 463: 223–244.
16. Kawai Y, Takami K, Shiosaka S, et al. Topographic localization of calcitonin gene-related peptide in the rat brain: an immunohistochemical analysis. *Neuroscience* 1985; 15: 747–763.
17. Li N, Liang J, Fang CY, et al. Involvement of CGRP and CGRPl receptor in nociception in the basolateral nucleus of amygdala of rats. *Neurosci Lett* 2008; 443: 184–187.
18. Lu YC, Chen YZ, Wei YY, et al. Neurochemical properties of the synapses between the parabrachial nucleus-derived CGRP-positive axonal terminals and the GABAergic neurons in the lateral capsular division of central nucleus of amygdala. *Mol Neurobiol* 2015; 51: 105–118.
19. Dong YL, Fukazawa Y, Wang W, et al. Differential postsynaptic compartments in the laterocapsular division of the central nucleus of amygdala for afferents from the parabrachial nucleus and the basolateral nucleus in the rat. *J Comp Neurol* 2010; 518: 4771–4791.
20. Han S, Soleiman MT, Soden ME, et al. Elucidating an affective pain circuit that creates a threat memory. *Cell* 2015; 162: 363–374.
21. Sato M, Ito M, Nagase M, et al. The lateral parabrachial nucleus is actively involved in the acquisition of fear memory in mice. *Mol Brain* 2015; 8: 22.
22. Han JS, Adwanikar H, Li Z, et al. Facilitation of synaptic transmission and pain responses by CGRP in the amygdala of normal rats. *Mol Pain* 2010; 6: 10.
23. Wu X, Zhang JTT, Liu J, et al. Calcitonin gene-related peptide erases the fear memory and facilitates long-term potentiation in the central nucleus of the amygdala in rats. *J Neurochem* 2015; 135: 787–798.
24. Nakao A, Takahashi Y, Nagase M, et al. Role of capsaicin-sensitive C-fiber afferents in neuropathic pain-induced synaptic potentiation in the nociceptive amygdala. *Mol Pain* 2012; 8: 51.
25. Watabe AM, Ochiai T, Nagase M, et al. Synaptic potentiation in the nociceptive amygdala following fear learning in mice. *Mol Brain* 2013; 6: 11.
26. Doods H, Hallermayer G, Wu D, et al. Pharmacological profile of BIBN4096BS, the first selective small molecule CGRP antagonist. *Br J Pharmacol* 2000; 129: 420–423.
27. Nagase M, Takahashi Y, Watabe AM, et al. On-site energy supply at synapses through monocarboxylate transporters maintains excitatory synaptic transmission. *J Neurosci* 2014; 34: 2605–2617.
28. Raman IM, Tong G and Jahr CE. Beta-adrenergic regulation of synaptic NMDA receptors by cAMP-dependent protein kinase. *Neuron* 1996; 16: 415–421.
29. Tong G, Shepherd D and Jahr CE. Synaptic desensitization of NMDA receptors by calcineurin. *Science* 1995; 267: 1510–1512.
30. Crump FT, Dillman KS and Craig AM. cAMP-dependent protein kinase mediates activity-regulated synaptic targeting of NMDA receptors. *J Neurosci* 2001; 21: 5079–5088.
31. Chen L and Huang LY. Protein-kinase-C reduces Mg2+ block of Nmda-receptor channels as a mechanism of modulation. *Nature* 1992; 356: 521–523.
32. Chen BS, Braud S, Badger JD, et al. Regulation of NR1/NR2C N-methyl-D-aspartate (NMDA) receptors by phosphorylation. *J Biol Chem* 2006; 281: 16583–16590.
33. Xu W, Lundeberg T, Wang YT, et al. Antinociceptive effect of calcitonin gene-related peptide in the central nucleus of amygdala: activating opioid receptors through amygdala-periaqueductal gray pathway. *Neuroscience* 2003; 118: 1015–1022.
34. Ehrlich I, Humeau Y, Grenier F, et al. Amygdala inhibitory circuits and the control of fear memory. *Neuron* 2009; 62: 757–771.
35. Simons LE, Pielech M, Erpelding N, et al. The responsive amygdala: treatment-induced alterations in functional connectivity in pediatric complex regional pain syndrome. *Pain* 2014; 155: 1727–1742.